Fullerene Nanostructures

DOI: 10.1002/ange.200904985

Controlled Fabrication of Fullerene C_{60} into Microspheres of Nanoplates through Porphyrin-Polymer-Assisted Self-Assembly**

*Xuan Zhang and Masayuki Takeuchi**

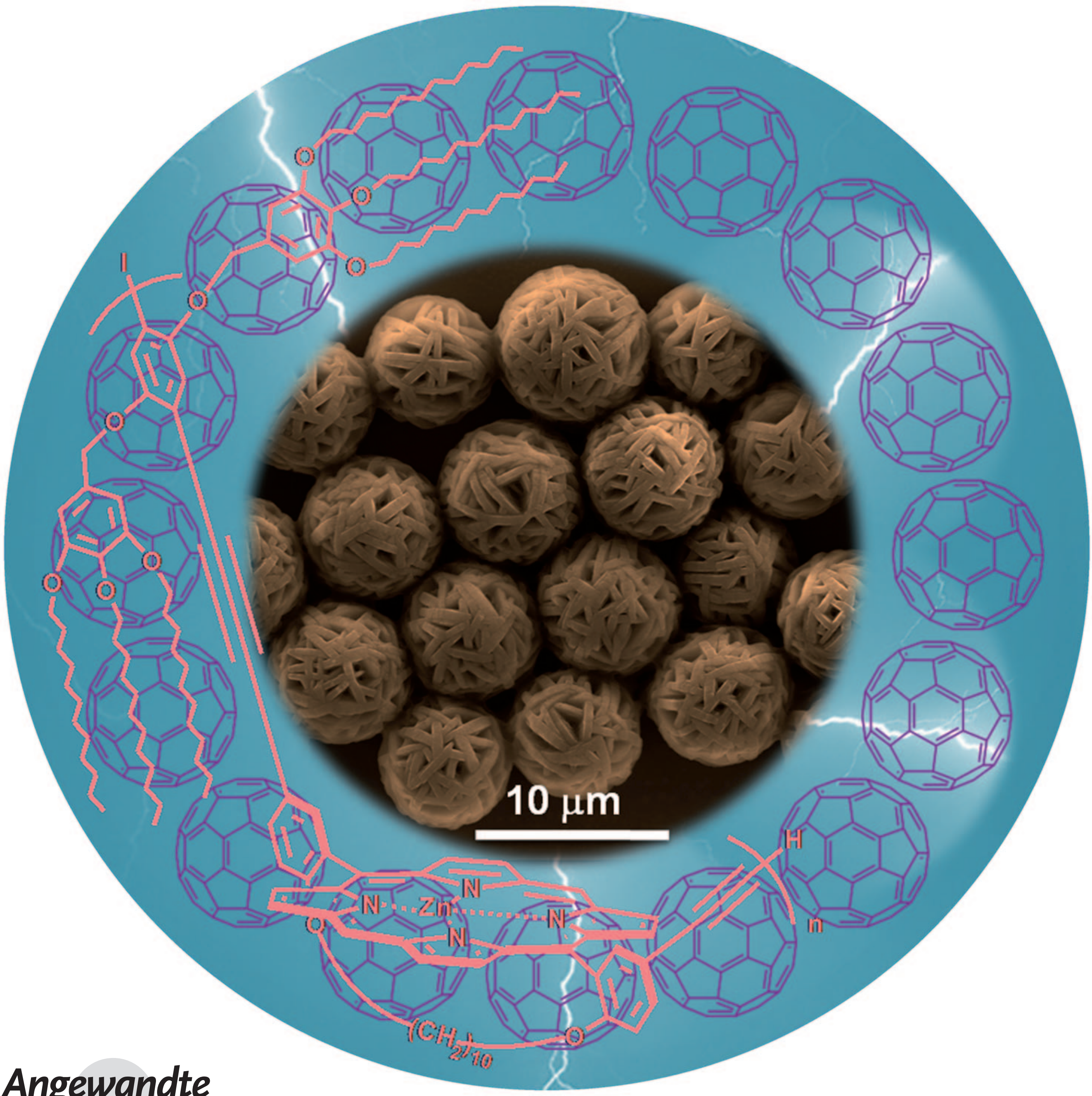

Fullerene (C_{60}) has drawn much attention in materials science because of its excellent electronic and mechanical properties.[1] C_{60} has many potential applications in various devices, such as photovoltaic cells,[2] organic transistors,[3] organic light-emitting diodes (OLEDs),[4] and sensors.[5] Recently, it has been recognized that the device performance, for example, the power conversion efficiency in a bulk heterojunction solar cell, strongly depends on the morphology of the photoactive C_{60} layer.[6] As a consequence, much effort has been devoted to the controlled construction of well-defined C_{60} nano- and microstructures. One-dimensional (1D) C_{60} rods,[7] wires,[8] whiskers,[9] tubes,[10] two-dimensional (2D) sheets,[11] and three-dimensional (3D) spheres[12] have been synthesized through the direct evaporation of solutions of pure C_{60} on substrates as well as by the template method,[10a] a solid–vapor process,[11c] a liquid–liquid interfacial precipitation method,[9c] and a reprecipitation method.[7d] These approaches, however, are usually accompanied by drawbacks on the limited modulation of shape and dimensionality, and particularly the fabrication of complex superstructures.

Self-assembly has proved to be an efficient approach to create hierarchical supramolecular architectures with controlled dimensionality and complex superstructures.[13] Recently, this technique has been applied successfully to the fabrication of supramolecular architectures of amphiphilic C_{60} derivatives,[14,15] wherein 1D fibers, 2D sheets, 3D spheres, and flowerlike objects were obtained in a controlled fashion from C_{60} derivatives bearing multiple alkyl chains.[15] Although the self-assembly of amphiphilic C_{60} derivatives has led to the fabrication of complex superstructures of novel shape, it is necessary to covalently attach multiple functional groups on the surface of C_{60} by chemical modification. Alternatively, the noncovalent functionalization of unmodified C_{60} by making a supramolecular composite would control the morphology and yet retain the intact C_{60} molecule. Whiskers and spheres have been obtained recently from a blend of C_{60} with poly(*p*-phenylene) derivatives;[16] however, the crystal structure of these objects was dominated by polymer packing. The controlled fabrication of architectures of unmodified C_{60} with complex superstructures is still a challenging task.

Herein we report that a porphyrin polymer[17] (**Por**, Scheme 1) was employed to control the assembly of C_{60} utilizing supramolecular interactions.[18] Unprecedentedly, well-defined 1D rods, 2D sheets, and complex 3D structures were successfully obtained from **Por**/C_{60} solutions under different experimental conditions. In particular, C_{60} microspheres comprising nanoplate structures with a face-centered cubic (*fcc*) structure and single-crystalline in nature were fabricated in a controllable fashion. Based on our analysis of captured intermediates, we propose a mechanism for the formation of C_{60} microspheres that resembles a bio-inspired mechanism of mineralization.

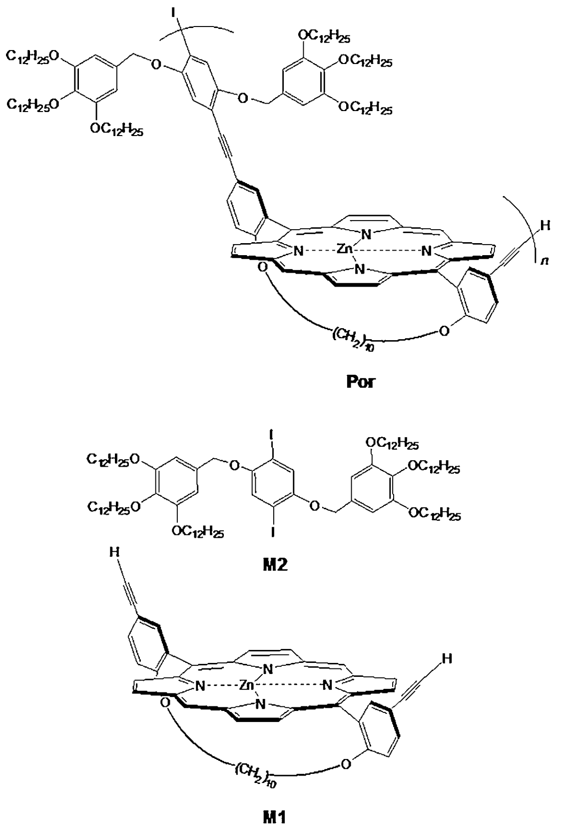

Scheme 1. Molecular structures of porphyrin polymer (**Por**) and related monomers (**M1** and **M2**). The number-average molecule mass (M_n) of **Por** is estimated as $M_n = 35\,000$ by comparison with a polystyrene standard.

Self-organized objects of supramolecular composites between **Por** and C_{60} were prepared by slow evaporation of a toluene solution of **Por** and C_{60} on a Si wafer under toluene atmosphere (see the Experimental Section). Figure 1 shows field emission scanning electron microscopy (FE-SEM) images of the objects obtained. Diverse micrometer-sized morphologies such as 1D rods and 2D sheets as well as 3D complex superstructures were obtained under different experimental conditions (see Figure 1 and Figure S1 in the Supporting Information). Evaporation of separate toluene solutions of pure C_{60} and **Por** provided rods and fibrous objects, respectively, whereas irregular-shaped aggregates formed from the solutions of C_{60} with the monomers **M1**, **M2**, or a mixture of **M1** and **M2** (Figure S2 in the Supporting Information). These results indicate that both C_{60} and the polymeric structure of **Por** contribute to the formation of these unique morphologies, which can be finely modulated by simply changing experimental conditions such as the weight ratio and the concentrations of **Por** and C_{60}.

When the weight ratio of **Por** to C_{60} (0.5 mg mL^{-1}, $[C_{60}] = 0.69$ mM) was fixed at 1:2 ($[\mathbf{Por}]_{unit}/[C_{60}] = 1{:}6$; $[\mathbf{Por}]_{unit}$

---

[*] Dr. X. Zhang, Dr. M. Takeuchi
Macromolecules Group, Organic Nanomaterials Center
National Institute for Materials Science
Tsukuba 305-0047 (Japan)
Fax: (+81) 29-859-2101
E-mail: takeuchi.masayuki@nims.go.jp

[**] We thank Dr. K. Sugiyasu and Dr. T. Nakanishi for valuable comments. This study was supported partially by KAKENHI (area 2107, 21108010 to M.T.) from the Ministry of Education, Culture, Science, Sports, and Technology (Japan).

Supporting information for this article is available on the WWW under http://dx.doi.org/10.1002/anie.200904985.

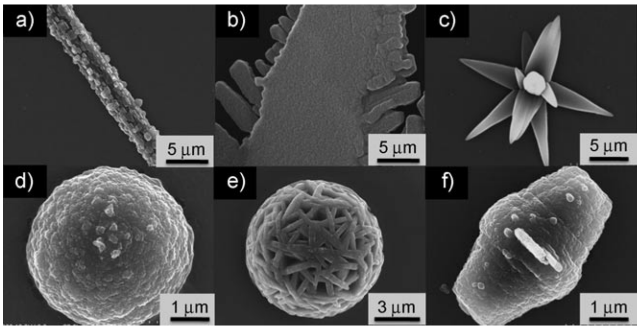

Figure 1. SEM images of diverse objects of **Por**–C_{60} blend obtained under different experimental conditions. Concentrations of C_{60} and **Por** (in mg mL^{-1}): a) 0.5, 0.05, b) 0.05, 0.05, c) 0.025, 0.25, d) 0.25, 0.25, e) 0.5, 0. 25, f) 0.75, 0.25, respectively.

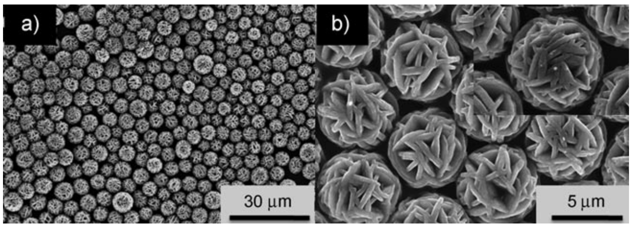

Figure 2. SEM images of C_{60} microspheres of nanoplates. Concentrations of C_{60} and **Por** (in mg mL^{-1}): 0.5 and 0.25, respectively.

denotes the concentration of a repeating unit of **Por** in the polymer shown in Scheme 1), highly monodisperse and uniform microspheres (average size ca. 5 µm) comprising nanoplates structures were predominantly obtained on the Si wafer (Figure 2), accompanied by disklike objects (Figure S3 in the Supporting Information). Energy-dispersive X-ray (EDX) spectroscopy analysis and element mapping revealed that carbon is the main component of the microspheres, as indicated by the prominent C peak; additional weak peaks reveal the presence of O and Zn in the objects, indicating the concomitance of **Por** in these microspheres (Figure S4 in the Supporting Information and vide infra). As shown in Figure 2, the microspheres range from 4–7 µm in diameter, and the platelike building units were revealed to be 200–300 nm thick from SEM images. Moreover, the size of the microspheres can be fine-tuned by changing the concentration of C_{60}. When the C_{60} concentration was increased from 0.25 to 0.5, 1.0, and 2.0 mg mL^{-1}, the average particle size increased from 3 to 5, 7, and 10 µm, respectively, while the weight ratio between **Por** and C_{60} was maintained at 1:2 (Figure S5 in the Supporting Information). When we diluted the C_{60} solution to 0.1 mg mL^{-1}, rodlike objects were mainly obtained.

Microspheres analogous to those obtained on the Si wafer were also found on other substrates such as glass, indium tin oxide coated glass, mica, and Al foil (Figure S6 in the Supporting Information). Remarkably, both disk and microsphere morphologies were also obtained from the slow evaporation of a **Por**/C_{60} solution in toluene at the air–water interface (Figure S7 in the Supporting Information), which enables us to transfer the resultant objects to any substrate such as a TEM grid (vide infra). These results indicate that the formation of microspheres is substrate-independent, and the objects can be prepared on different substrates for various applications. In addition, neither light nor the water content of the toluene solvent affected the resultant morphology; similar microspheres composed of nanoplates were obtained in the dark and also from water-saturated toluene solution. In contrast, the drying speed, temperature, and solvent for the **Por**/C_{60} blend strongly influence the resultant morphologies. The microsphere morphology dominated only when the drying process continued over 10 hours under a saturated toluene atmosphere (see Figure S8 in the Supporting Information). Without sufficient toluene vapor, disklike objects were mainly formed, suggesting that these objects are intermediates. Meanwhile, the microsphere objects were obtained in the temperature range of 15–26 °C; at either lower (10 °C) or higher (30 °C) temperatures, or with other solvents such as benzene and *p*-xylene, we did not observe microspheres on the Si surface.

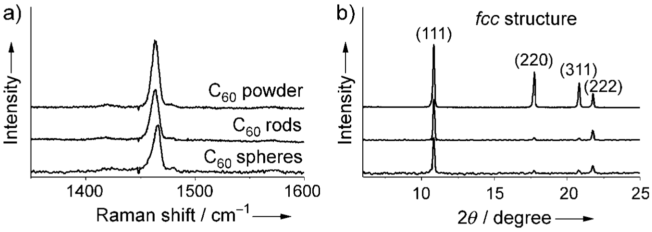

Figure 3. Raman spectra (a) and XRD patterns (b) of C_{60} powder, rods, and microspheres.

To obtain further insight into how C_{60} and **Por** organize in the microspheres, we conducted Raman spectroscopy, X-ray diffraction (XRD), and transmission electron microscopy (TEM). Figure 3 a shows Raman spectra recorded for microspheres on a Si wafer. The corresponding spectra of C_{60} rods obtained without **Por** under the same conditions and untreated C_{60} powder are also shown for comparison. The characteristic band for the $A_g(2)$ pentagonal pinch mode in the Raman spectra around 1460 cm^{-1} was observed for all of microspheres, C_{60} rods, and untreated C_{60} (Figure 3 a). This indicates that only monomeric C_{60} molecules are involved in these objects because the $A_g(2)$ line shifts to lower frequency in polymerized C_{60}.[19] It should be noted, however, that the $A_g(2)$ band showed a substantial 3 cm^{-1} shift for microspheres (1466 cm^{-1}) relative to those observed for C_{60} rods and untreated C_{60} (both at 1463 cm^{-1}). This shift may be attributed to supramolecular interactions between the porphyrin polymer and C_{60}. X-ray diffraction (XRD) patterns for microspheres recorded on a Si substrate are shown in Figure 3 b. The well-defined XRD patterns of the microspheres match very well with those of C_{60} rods and untreated C_{60}. Thus these patterns were readily assigned as a classic *fcc* structure: four strong peaks are indexed as (111), (220), (311), and (222) from the *fcc* lattices, indicating that the microspheres have pure *fcc* crystal structure. In contrast, previously obtained C_{60} crystals usually have a mixed phase of the *fcc* and hexagonal structures.[9,10a,11a,b]

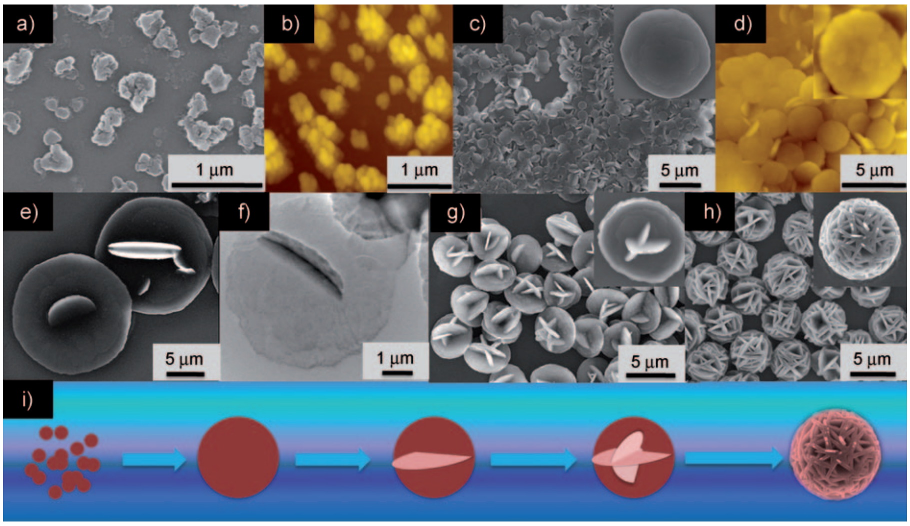

Figure 5. Studies on the plausible mechanism for the formation of C_{60} microspheres. SEM (a) and AFM (b) images of particles obtained after fast drying within 1 min in air. SEM (c) and AFM (d) images of disks obtained under less toluene vapor and dried within 6 h. SEM (e, g) and TEM (f) images of disklike intermediate objects. h) SEM images of ball-shaped microspheres. (i) Plausible mechanism for the formation of C_{60} microspheres from multilayer disks of nanoparticle aggregates.

As the obtained microspheres are too large to observe by TEM, disklike intermediates were characterized by this method. TEM samples were prepared by direct evaporation of toluene solutions of **Por**/C_{60} on a carbon-coated Cu grid (Figure 4 and Figure S9 in the Supporting Information) or by transferring objects formed at the air–water interface to a grid (Figure S10 in the Supporting Information). Figure 4 shows TEM and high-resolution TEM (HR-TEM) images of disklike objects. The selected area electron diffraction (SAED) patterns show regular hexagonal diffraction spots, and we confirm that these objects are single-crystalline in nature (inset in Figure 4 a). The HR-TEM image recorded near the edge of the disk indicates well-defined lattice fringes with an interplanar spacing of 0.81 nm (Figure 4 b), which matches well with the XRD result (Figure 3 b) and corresponds to the diameter of C_{60}.

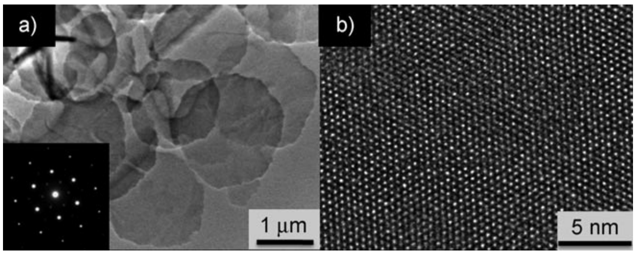

Figure 4. TEM (a) and HR-TEM (b) images of C_{60} disks. The inset in (a) shows the SAED pattern.

The capture of intermediate objects enabled us to understand the assembly procedure. The drying process was controlled by the amount of toluene vapor in order to capture intermediate structures. We noticed that small particle aggregates 20–200 nm in height and 200–500 nm in diameter (according to AFM measurements) were mainly obtained when a toluene solution of **Por**/C_{60} (1:2 weight ratio) was dried within 1 min in air without toluene vapor or by spin-coating on a Si substrate (Figure 5 a, b, and Figure S11 in the Supporting Information).

When the **Por**/C_{60} solution was dried within 6 hours under less toluene vapor (200 μL), micrometer-sized multilayer disks with a thickness of 40–200 nm and a diameter of 2.5 μm were predominantly obtained (Figure 5 c–f and Figure S12 in the Supporting Information). Moreover, with an excess of toluene vapor (500 μL), the **Por**/C_{60} solution dried completely over 10 hours and microspheres were predominantly observed accompanied by disk- or incomplete ball-like objects (Figure 5 g, h and Figures S3 and S8 in the Supporting Information). Based on these results, we propose a process for microsphere growth (Figure 5 i). During the slow evaporation of the homogeneous composite solution, the initially formed nanoparticle aggregates assemble to form a micrometer-sized multilayer disk. This intermediate structure provides a platform for the formation of another disk composed of freshly formed nanoparticle aggregates perpendicular to the initial platform; finally a complex microsphere of nanoplates is constructed by an oriented-attachment growth mechanism.[20] The oriented-attachment process involves the spontaneous self-organization of adjacent particles to share a common crystallographic orientation, and subsequent fusion of these particles at a planar interface.[20]

We infer that **Por** plays multiple roles in the present system, such as interacting with C_{60} to preorganize C_{60} molecules around polymer chain by molecular recognition and then assisting in the self-assembly of C_{60} molecules to disklike objects and microspheres.[21] It is noteworthy to mention that EDX analysis (Figure S4 in the Supporting Information) clearly indicates that the microspheres contain only minor amounts of **Por** (the Zn/C atomic ratio is 1:1357, corresponding ca. $[\mathbf{Por}]_{unit}/[C_{60}] = 1{:}20$). This could be tentatively explained by the exclusion of **Por** during the formation of crystals C_{60}. This step resembles stages in bio-inspired mineralization,[22] where polymer additives exert a powerful influence on crystal growth and the self-assembly of superstructures but are predominantly excluded from the crystalline phase.[22,23] This approach has been used extensively for the synthesis of inorganic crystals having complex shapes and was also recently extended to the synthesis and crystallization of organic dyes.[24]

In conclusion, novel C_{60} microspheres composed of nanoplates have been fabricated by porphyrin-polymer-assisted supramolecular self-assembly. We have shown that the obtained C_{60} microspheres are single-crystalline and exhibit pure *fcc* structure; this is a rare example of a hierarchical supramolecular architecture with a complex superstructure fabricated from the self-assembly of unmodified C_{60}. The possible formation mechanism was also described based on the analysis of captured intermediates. Namely, the oriented attachment of initially formed nanoparticles leads to the growth of micrometer-sized disks, providing a platform for further disk growth and final transformation into microspheres. The porphyrin polymer **Por** was speculated to play multiple roles such as preorganizing and assisting the self-assembly of C_{60} molecules in a "programmed" fashion to form microspheres; it is then excluded from the crystalline phase. The approach we have presented in this study paves the way to the fabrication of new complex supramolecular architectures of fullerenes as well as other organic molecules by employing various functional polymers.

Experimental Section

C_{60} (purity 99%) and toluene (anhydrous) were purchased from Aldrich and Wako and used as received. The detailed synthesis of the porphyrin polymer is described in the Supporting Information.

The typical procedure for the synthesis of C_{60} microspheres is briefly described as follows: 20 µL C_{60} stock solution (1 mg mL^{-1} in toluene) was mixed with 10 µL **Por** stock solution (1 mg mL^{-1} in toluene) and diluted with 10 µL toluene in a 1 mL vial; 20 µL of this blend solution was transferred to a Si wafer (10 mm × 10 mm) and slowly evaporated in a glass petri dish (diameter 95, height 20 mm) under 500 µL toluene; the Si wafer had been simply rinsed with acetone and dried in air before use.

Received: September 5, 2009

Keywords: fullerenes · nanostructures · polymers · self-assembly · supramolecular chemistry

---

[1] a) H. W. Kroto, J. R. Heath, S. C. O'Brien, R. F. Curl, R. E. Smalley, *Nature* **1985**, *318*, 162–163; b) A. Cravino, N. S. Sariciftci, *J. Mater. Chem.* **2002**, *12*, 1931–1943; c) D. M. Guldi, B. M. Illescas, C. M. Atienza, M. Wielopolski, N. Martin, *Chem. Soc. Rev.* **2009**, *38*, 1587–1597.

[2] For solar cells: a) G. Yu, J. Gao, J. C. Hummelen, F. Wudl, A. J. Heeger, *Science* **1995**, *270*, 1789–1791; b) J. Y. Kim, K. Lee, N. E. Coates, D. Moses, T.-Q. Nguyen, M. Dante, A. J. Heeger, *Science* **2007**, *317*, 222–225; c) G. Li, V. Shrotriya, J. Huang, Y. Yao, T. Moriarty, K. Emery, Y. Yang, *Nat. Mater.* **2005**, *4*, 864–868; d) B. C. Thompson, J. M. J. Frechet, *Angew. Chem.* **2008**, *120*, 62–82; *Angew. Chem. Int. Ed.* **2008**, *47*, 58–77.

[3] For transistors: a) C. D. Dimitrakopoulos, P. R. Malenfant, *Adv. Mater.* **2002**, *14*, 99–117; b) K. Itaka, M. Yamashiro, J. Yamaguchi, M. Haemori, S. Yaginuma, Y. Matsumoto, M. Kondo, H. Koinuma, *Adv. Mater.* **2006**, *18*, 1713–1716; c) A. L. Briseno, S. C. B. Mannsfeld, M. M. Ling, S. Liu, R. J. Tseng, C. Reese, M. E. Roberts, Y. Yang, F. Wudl, Z. Bao, *Nature* **2006**, *444*, 913–917; d) C. Yang, S. Cho, A. J. Heeger, F. Wudl, *Angew. Chem.* **2009**, *121*, 1620–1623; *Angew. Chem. Int. Ed.* **2009**, *48*, 1592–1595.

[4] For OLEDs: a) Y. Y. Yuan, S. Han, D. Grozea, Z. H. Lu, *Appl. Phys. Lett.* **2006**, *88*, 093503; b) F. D'Souza, E. Maligaspe, M. E. Zandler, N. K. Subbaiyan, K. Ohkubo, S. Fukuzumi, *J. Am. Chem. Soc.* **2008**, *130*, 16959–16967.

[5] For sensors: a) G. Yu, J. Wang, J. McElvain, A. J. Heeger, *Adv. Mater.* **1998**, *10*, 1431–1434; b) R. N. Goyal, V. K. Gupta, N. Bachheti, *Anal. Chim. Acta* **2007**, *597*, 82–89; c) S. Nagl, C. Baleizao, S. M. Borisov, M. Schäferling, M. N. Berberan-Santos, O. S. Wolfbeis, *Angew. Chem.* **2007**, *119*, 2368–2371; *Angew. Chem. Int. Ed.* **2007**, *46*, 2317–2319.

[6] a) M. Campoy-Quiles, T. Ferenczi, T. Agostinelli, P. G. Etchegoin, Y. Kim, T. D. Anthopoulos, P. N. Stavrinou, D. D. C. Bradley, J. Nelson, *Nat. Mater.* **2008**, *7*, 158–164; b) H. Hoppe, N. S. Sariciftci, *J. Mater. Chem.* **2006**, *16*, 45–61; c) J. Peet, M. L. Senatore, A. J. Heeger, G. C. Bazan, *Adv. Mater.* **2009**, *21*, 1521–1527.

[7] For C_{60} rods: a) L. Wang, B. Liu, D. Liu, M. Yao, Y. Hou, S. Yu, T. Cui, D. Li, G. Zou, A. Iwasiewicz, B. Sundqvist, *Adv. Mater.* **2006**, *18*, 1883–1886; b) H.-X. Ji, J.-S. Hu, L.-J. Wan, Q.-X. Tang, W.-P. Hua, *J. Mater. Chem.* **2008**, *18*, 328–332; c) Y. Jin, R. J. Curry, J. Sloan, R. A. Hatton, L. C. Chong, N. Blanchard, V. Stolojan, H. W. Krotob, S. R. P. Silva, *J. Mater. Chem.* **2006**, *16*, 3715–3720; d) Z. Tan, A. Masuhara, H. Kasai, H. Nakanishi, H. Oikawa, *Jpn. J. Appl. Phys.* **2008**, *47*, 1426–1428.

[8] For C_{60} wires: a) J. Geng, W. Zhou, P. Skelton, W. Yue, I. A. Kinloch, A. H. Windle, B. F. G. Johnson, *J. Am. Chem. Soc.* **2008**, *130*, 2527–2534; b) Y.-G. Guo, C.-J. Li, L.-J. Wan, D.-M. Chen, C.-R. Wang, C.-L. Bai, Y.-G. Wang, *Adv. Funct. Mater.* **2003**, *13*, 626–630; c) R. Bai, M. Ouyang, Z.-Z. Li, L.-G. Yang, M.-M. Shi, G. Wu, M. Wang, H.-Z. Chen, *J. Mater. Chem.* **2008**, *18*, 4318–4323.

[9] For C_{60} whiskers: a) M. Sathish, K. Miyazawa, T. Sasaki, *Chem. Mater.* **2007**, *19*, 2398–2400; b) J. Minato, K. Miyazawa, *Carbon* **2005**, *43*, 2837–2841; c) K. Miyazawa, Y. Kuwasaki, A. Obayashi, K. Kuwabara, *J. Mater. Res.* **2002**, *17*, 83–88.

[10] For C_{60} tubes: a) H. B. Liu, Y. L. Li, L. Jiang, H. Y. Luo, S. Q. Xiao, H. J. Fang, H. M. Li, D. B. Zhu, D. P. Yu, J. Xu, B. Xiang, *J. Am. Chem. Soc.* **2002**, *124*, 13370–13371; b) K. Miyazawa, J. Minato, T. Yoshii, M. Fujino, T. Suga, *J. Mater. Res.* **2005**, *20*, 688–695.

[11] For C_{60} sheets: a) M. Sathish, K. Miyazawa, *J. Am. Chem. Soc.* **2007**, *129*, 13816–13817; b) M. Sathish, K. Miyazawa, J. P. Hill, K. Ariga, *J. Am. Chem. Soc.* **2009**, *131*, 6372–6373; c) H. S. Shin, S. M. Yoon, Q. Tang, B. Chon, T. Joo, H. C. Choi, *Angew. Chem.* **2008**, *120*, 705–708; *Angew. Chem. Int. Ed.* **2008**, *47*, 693–696.

[12] For C_{60} spheres: A. Masuhara, Z. Tan, H. Kasai, H. Nakanishi, H. Oikawa, *Jpn. J. Appl. Phys.* **2009**, *48*, 050206–050208.

[13] a) J.-M. Lehn, *Science* **2002**, *295*, 2400–2403; b) J. A. A. W. Elemans, A. E. Rowan, R. J. M. Nolte, *J. Mater. Chem.* **2003**, *13*, 2661–2670; c) F. J. M. Hoeben, P. Jonkheijm, E. W. Meijer, A. P. H. J. Schenning, *Chem. Rev.* **2005**, *105*, 1491–1546; d) K. Sada, M. Takeuchi, N. Fujita, M. Numata, S. Shinkai, *Chem. Soc. Rev.* **2007**, *36*, 415–435; e) K. Ariga, J. P. Hill , M. V. Lee, A. Vinu, R. Charvet, S. Acharya, *Sci. Technol. Adv. Mater.* **2008**, *9*, 014109.

[14] a) S. Zhou, C. Burger, B. Chu, M. Sawamura, N. Nagahama, M. Toganoh, U. E. Hackler, H. Isobe, E. Nakamura, *Science* **2001**, *291*, 1944–1947; b) N. Nakashima, T. Ishii, M. Shirakusa, T. Nakanishi, H. Murakami, T. Sagara, *Chem. Eur. J.* **2001**, *7*, 1766–1772; c) V. Georgakilas, F. Pellarini, M. Prato, D. M. Guldi, M. Melle-Franco, F. Zerbetto, *Proc. Natl. Acad. Sci. USA* **2002**, *99*, 5075–5080; d) N. Fujita, T. Yamashita, M. Asai, S. Shinkai, *Angew. Chem.* **2005**, *117*, 1283–1287; *Angew. Chem. Int. Ed.* **2005**, *44*, 1257–1261; e) R. Charvet, D.-L. Jiang, T. Aida, *Chem. Commun.* **2004**, 2664–2665; f) D. M. Guldi, F. Zerbetto, V. Georgakilas, M. Prato, *Acc. Chem. Res.* **2005**, *38*, 38–43; g) R. Tsunashima, S. Noro, T. Akutagawa, T. Nakamura, H. Kawakami, K. Toma, *Chem. Eur. J.* **2008**, *14*, 8169–8176.

[15] a) T. Nakanishi, W. Schmitt, T. Michinobu, D. Kurth, K. Ariga, *Chem. Commun.* **2005**, 5982 – 5984; b) T. Nakanishi, K. Ariga, T. Michinobu, K. Yoshida, H. Takahashi, T. Teranishi, H. Mohwald, D. G. Kurth, *Small* **2007**, *3*, 2019 – 2023; c) T. Nakanishi, T. Michinobu, K. Yoshida, N. Shirahata, K. Ariga, H. Moehwald, D. G. Kurth, *Adv. Mater.* **2008**, *20*, 443 – 446; d) Y. Shen, J. Wang, U. Kuhlmann, P. Hildebrandt, K. Ariga, H. Möhwald, D. G. Kurth, T. Nakanishi, *Chem. Eur. J.* **2009**, *15*, 2763 – 2767; e) J. Wang, Y. Shen, S. Kessel, P. Ferandes, K. Yoshida, S. Yagai, D. G. Kurth, H. Möhwald, T. Nakanishi, *Angew. Chem.* **2009**, *121*, 2200 – 2204; *Angew. Chem. Int. Ed.* **2009**, *48*, 2166 – 2170; f) T. Nakanishi, N. Miyashita, T. Michinobu, Y. Wakayama, T. Tsuruoka, K. Ariga, D. Kurth, *J. Am. Chem. Soc.* **2006**, *128*, 6328 – 6329.

[16] a) M. H. Nurmawati, P. K. Ajikumar, R. Renu, C. H. Sow, S. Valiyaveettil, *ACS Nano* **2008**, *2*, 1429 – 1436; b) M. H. Nurmawati, P. K. Ajikumar, L. A. Heng, H. R. Li, S. Valiyaveettil, *Chem. Commun.* **2008**, 4945 – 4947.

[17] M. Takeuchi, C. Fujikoshi, Y. Kubo, K. Kaneko, S. Shinkai, *Angew. Chem.* **2006**, *118*, 5620 – 5625; *Angew. Chem. Int. Ed.* **2006**, *45*, 5494 – 5499.

[18] a) M. Ayabe, A. Ikeda, Y. Kubo, M. Takeuchi, S. Shinkai, *Angew. Chem.* **2002**, *114*, 2914 – 2916; *Angew. Chem. Int. Ed.* **2002**, *41*, 2790 – 2792; b) H. Nobukuni, Y. Shimazaki, F. Tani, Y. Naruta, *Angew. Chem.* **2007**, *119*, 9133 – 9136; *Angew. Chem. Int. Ed.* **2007**, *46*, 8975 – 8978; c) P. D. W. Boyd, C. A. Reed, *Acc. Chem. Res.* **2005**, *38*, 235 – 242; d) K. Tashiro, T. Aida, *Chem. Soc. Rev.* **2007**, *36*, 189 – 197; For porphyrin/C_{60}-based devices: e) T. Hasobe, H. Imahori, P. V. Kamat, T. K. Ahn, S. K. Kim, D. Kim, A. Fujimoto, T. Hirakawa, S. Fukuzumi, *J. Am. Chem. Soc.* **2005**, *127*, 1216 – 1228; f) H. Imahori, T. Umeyama, *J. Phys. Chem. C* **2009**, *113*, 9029 – 9039; g) S. A. Vail, P. J. Krawczuk, D. M. Guldi, A. Palkar, L. Echegoyen, J. P. C. Tomé, M. A. Fazio, D. I. Schuster, *Chem. Eur. J.* **2005**, *11*, 3375 – 3388.

[19] H. Kuzmany, R. Pfeiffer, M. Hulman, C. Kramberger, *Philos. Trans. R. Soc. London Ser. A* **2004**, *362*, 2375 – 2406.

[20] a) R. L. Penn, J. F. Banfield, *Science* **1998**, *281*, 969 – 971; b) R. L. Penn, J. F. Banfield, *Geochim. Cosmochim. Acta* **1999**, *63*, 1549 – 1557; c) J. F. Banfield, S. A. Welch, H. Zhang, T. T. Ebert, R. L. Penn, *Science* **2000**, *289*, 751 – 754; d) M. Niederberger, H. Cölfen, *Phys. Chem. Chem. Phys.* **2006**, *8*, 3271 – 3287.

[21] To confirm the supramolecular interactions between the porphyrin polymer and C_{60}, we investigated the photophysical change of the **Por**–C_{60} blend in toluene. Upon addition of C_{60}, small red-shift of the Soret band (up to 2 nm) in the absorption spectra of porphyrin was observed, while the porphyrin fluorescence was significantly quenched (Figure S13 in the Supporting Information). These photophysical changes resemble those generally observed in porphyrin–fullerene host–guest systems, supporting the existence of intermolecular interactions, most likely π–π and van der Waals interactions, and efficient electron transfer between the porphyrin-polymer donor and the C_{60} acceptor.[18c]

[22] a) S. Mann, D. D. Archibald, J. M. Didymus, T. Douglas, B. R. Heywood, F. C. Meldrum, N. J. Reeves, *Science* **1993**, *261*, 1286 – 1292; b) A.-W. Xu, Y. Ma, H. Cölfen, *J. Mater. Chem.* **2007**, *17*, 415 – 449.

[23] Another explanantion for the minor amount of **Por** in the microspheres is the partial use of **Por** in making composites with C_{60}. Most likely, **Por** suppresses the crystal growth of a certain axis of C_{60}, although the detailed role of **Por** is still not clear for us at this stage.

[24] Y. Ma, G. M. Mehltretter, C. Plug, N. Rademacher, M. U. Schmidt, H. Cölfen, *Adv. Funct. Mater.* **2009**, *19*, 2095 – 2101.